β-Decay Half-Lives of 110 Neutron-Rich Nuclei across the N=82 Shell Gap: Implications for the Mechanism and Universality of the Astrophysical r Process

G. Lorusso *et al.*

Phys. Rev. Lett. **114**, 192501 — Published 11 May 2015

DOI: 10.1103/PhysRevLett.114.192501

β-Decay Half-lives of 108 Neutron-Rich Nuclei across the $N = 82$ Shell Gap: Implications for the Mechanism and Universality of the r-process

G. Lorusso,[1,2,3] S. Nishimura,[1,4] Z.Y. Xu,[1,5,6] A. Jungclaus,[7] F. Browne,[1,8] P. Doornenbal,[1] G. Gey,[1,9] H.S. Jung,[10] B. Meyer,[11] G.S. Simpson,[9] Y. Shimizu,[1] P.-A. Söderström,[1] T. Sumikama,[12] P. Schury,[1] J. Taprogge,[1,7,13] Zs.Vajta,[1,14] H. Watanabe,[1,15] J. Wu,[1,16] H. Baba,[1] G. Benzoni,[17] K.Y. Chae,[18] F.C.L. Crespi,[17,19] N. Fukuda,[1] R. Gernhäuser,[20] N. Inabe,[1] T. Isobe,[1] T. Kajino,[4,21] D. Kameda,[1] G.D. Kim,[22] Y.-K. Kim,[22] I. Kojouharov,[23] F.G. Kondev,[24] T. Kubo,[1] N. Kurz,[23] Y.K. Kwon,[22] G.J. Lane,[25] Z. Li,[16] A. Montaner-Pizá,[26] K. Moschner,[27] F. Naqvi,[28] M. Niikura,[29] H. Nishibata,[30] A. Odahara,[30] R. Orlandi,[31] Z. Patel,[3] Zs. Podolyák,[3] H. Sakurai,[1,29] H. Schaffner,[23] S. Shibagaki,[4,32] K. Steiger,[20] H. Suzuki,[1] H. Takeda,[1] A. Wendt,[27] A. Yagi,[30] and K. Yoshinaga[33]

[1]*RIKEN Nishina Center, 2-1 Hirosawa, Wako-shi, Saitama 351-0198, Japan*
[2]*National Physics Laboratory, Teddington, Middlesex TW11 0LW, UK*
[3]*Department of Physics, University of Surrey, Guildford, GU2 7XH, UK*
[4]*Division of Theoretical Astronomy, NAOJ, 181-8588 Mitaka, Japan*
[5]*Department of Physics, University of Tokyo, Hongo, Bunkyo-ku, Tokyo 113-0033, Japan*
[6]*Department of Physics, the University of Hong Kong, Pokfulam Road, Hong Kong*
[7]*Instituto de Estructura de la Materia, CSIC, E-28006 Madrid, Spain*
[8]*School of Computing, Engineering and Mathematics, University of Brighton, Brighton BN2 4JG, United Kingdom*
[9]*LPSC, Université Joseph Fourier Grenoble 1, CNRS/IN2P3, Institut National Polytechnique de Grenoble, F-38026 Grenoble Cedex, France*
[10]*Department of Physics, Chung-Ang University, Seoul 156-756, Republic of Korea*
[11]*Department of Physics and Astronomy, Clemson University, Clemson, South Carolina 29634, USA*
[12]*Department of Physics, Tohoku University, Aoba, Sendai, Miyagi 980-8578, Japan*
[13]*Departamento de Física Teórica, Universidad Autónoma de Madrid, E-28049 Madrid, Spain*
[14]*Institute for Nuclear Research, Hungarian Academy of Sciences, P. O. Box 51, Debrecen, H-4001, Hungary*
[15]*IRCNPC, School of Physics and Nuclear Energy Engineering, Beihang University, Beijing 100191, China*
[16]*Department of Physics, Peking University, Beijing 100871, China*
[17]*INFN Sezione di Milano, I-20133 Milano, Italy*
[18]*Department of Physics, Sungkyunkwan University, Suwon 440-746, Republic of Korea*
[19]*Dipartimento di Fisica, Università di Milano, I-20133 Milano, Italy*
[20]*Physik Department E12, Technische Universität München, D-85748 Garching, Germany*
[21]*Department of Astronomy, University of Tokyo, Hongo, Bunkyo-ku, Tokyo 113-0033, Japan*
[22]*Institute for Basic Science, Rare Isotope Science Project, Yuseong-daero 1689-gil, Yuseong-gu, 305-811 Daejeon, Republic of Korea*
[23]*GSI Helmholtzzentrum für Schwerionenforschung GmbH, 64291 Darmstadt, Germany*
[24]*Nuclear Engineering Division, Argonne National Laboratory, Argonne, Illinois 60439, USA*
[25]*Department of Nuclear Physics, R.S.P.E., Australian National University, Canberra, A.C.T. 0200, Australia*
[26]*Instituto de Física Corpuscular, CSIC-University of Valencia, E-46980 Paterna, Spain*
[27]*Institut für Kernphysik, Universität zu Köln, Zülpicher Strasse 77, D-50937 Köln, Germany*
[28]*Wright Nuclear Structure Laboratory, Yale University, New Haven, CT 06520-8120, USA*
[29]*Department of Physics and Astronomy, University of Tokyo, Hongo, Bunkyo-ku, Tokyo 113-0033, Japan*
[30]*Department of Physics, Osaka University, Machikaneyama-machi 1-1, Osaka 560-0043Toyonaka, Japan*
[31]*Instituut voor Kern en Stralingsfysica, KU Leuven, University of Leuven, B-3001 Leuven, Belgium*
[32]*Department of Astronomy, The University of Tokyo, 113-033 Tokyo, Japan*
[33]*Department of Physics, Tokyo University of Science, 2641 Yamazaki, Noda, Chiba 278-8510, Japan*

The β-decay half-lives of 108 neutron-rich isotopes of the elements from $_{37}$Rb to $_{50}$Sn were measured at the Radioactive Isotope Beam Factory (RIBF). The 41 new half-lives follow robust systematics and highlight the persistence of shell effects. The new data have direct implications for r-process calculations and reinforce the notion that the second ($A \approx 130$) and the rare-earth-element ($A \approx 160$) abundance peaks may result from the freezout of an $(n, \gamma) \rightleftarrows (\gamma, n)$ equilibrium. In such equilibrium, the new half-lives are likely to determine the abundance of rare-earth elements, allowing for a more reliable discussion of the r-process universality. It is anticipated that universality may not extend to the elements Sn, Sb, I, and Cs, making the detection of these elements in metal-poor stars of the utmost importance to determine the exact conditions of individual r-process events.

Introduction.—The origin of the heavy elements from iron to uranium is one of the main open questions in science. The slow neutron-capture (s-) process of nucleosynthesis [1, 2], occurring primarily in helium-burning zones of stars, produces about half of the heavy element abundance in the universe. The remaining half requires a more violent process known as the rapid neutron-capture (r-) process [3–5]. During the r-process, in environments

of extreme temperatures and neutron densities, a reaction network of neutron captures and β decays synthesizes very neutron-rich isotopes in a fraction of a second. These isotopes, upon exhaustion of the supply of free neutrons, decay into the stable or semistable isotopes observed in the solar system. However, none of the proposed stellar models including different stages of core-collapse supernovae [6–11] and merging neutron stars [12–15] can fully explain abundance observations. The mechanism of the r-process is also uncertain. At temperatures of one billion degrees or more, photons can excite unstable nuclei which then emit neutrons, thus counteracting neutron captures in an $(n,\gamma) \rightleftarrows (\gamma,n)$ equilibrium that determines the r-process. These conditions are expected in neutrino-driven wind environments that include the collapse of a supernova core and the accreting torus formed around the black hole remnant of neutron star mergers. Alternatively, recent r-process models have shown that the r-process is possible also at lower temperatures or higher neutron densities where the contribution from (γ,n) reactions is minor. These conditions are expected in supersonically expanding neutrino-driven outflow in low-mass supernovae progenitors (e.g., 8-12 $M_\odot$) or prompt ejecta from neutron star mergers [16]. The final abundance distribution may also be dominated by post-processing effects such as fission of heavy nuclei ($A \gtrsim 280$) possibly produced in neutron star mergers [17].

New clues about the r-process have come from the discovery of detailed elemental distributions in some metal-poor stars in the halo of our galaxy [18, 19]. A main conclusion of these observations is that the abundance pattern of the elements between barium (Ba, proton number $Z = 56$) and hafnium (Hf, $Z = 78$) is universal. Recent observations by the Space Telescope Imaging Spectrograph on board of the Hubble Space Telescope [20, 21] indicate that also tellurium (Te, $Z = 52$) is robustly produced along with the rare earth elements.

Nuclear physics properties such as β-decay half-lives and masses are key to predict abundance pattern and extract signatures of the r-process from a detailed comparison to astronomical observations [22]. This is specially true when $(n,\gamma) \rightleftarrows (\gamma,n)$ equilibrium is established. Otherwise, (n,γ) cross sections or fission properties may very well be responsible for the main abundance observations. In this letter we report on the half-life measurement of 108 unstable nuclei with proton number $Z \leq 50$ and neutron number $N \approx 82$. These nuclei are key in any r-process mechanism [22] because their enhanced binding *bends* the r-process path closer to stability slowing down the reaction flow – the flow has to wait at the slowly decaying species. The half-lives of these *waiting-point* nuclei determine the time scale of the r-process and shape the prominent r-process abundance peak of isotopes with $A \approx 130$. The precise theoretical prediction of these half-lives is challenging because the structure evolution of $N \approx 82$ is still unknown despite the recent experimental efforts [23–28]. The data we present in this letter serve also as important constrain to probe and improve nuclear models in this region.

Experimental procedure.—The nuclei of interest were produced by fission of a ^{238}U beam induced through collisions with a beryllium target. The U beam had an energy of 345A MeV and an average intensity of about 6×10^{10} ions/s. After selection and identification, exotic nuclei were implanted at a rate of 50 ions/s in the stack of eight double-sided silicon strip detectors WAS3ABi [29], surrounded by the 84 high-purity germanium detectors of the EURICA array [30] to detect γ radiation from the excited reaction products. The particle identification spectrum of the isotopes delivered to the decay station is shown in Fig. 1. Implanted ions and subsequent electrons emitted in the ions' β decays were correlated in time and position to build decay curves and extract half-lives using the analysis method detailed in Ref. [31].

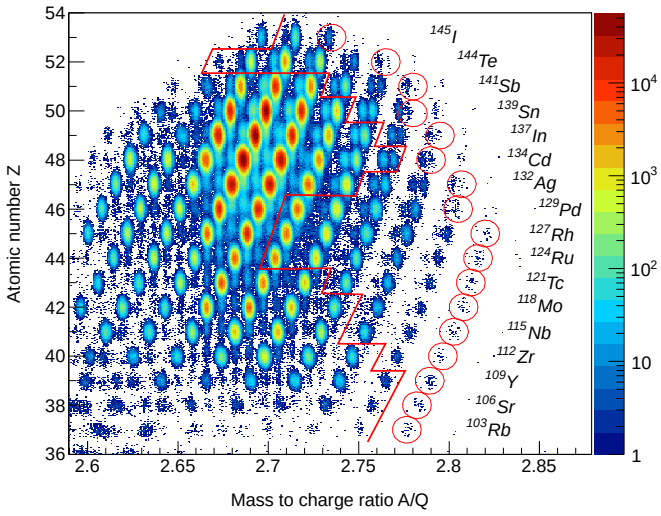

FIG. 1: (color online) Particle identification spectrum [32]. Ions are identified with respect to proton number Z and the mass-to-charge ratio A/Q. Charge state contamination is significant but well separated in A/Q for the nuclei of interest. Nuclei with newly measured half-lives are on the right side of the red solid line. The heaviest masses for which half-lives can be measured are tagged for reference by red circles. The half-lives reported in this article are for the elements from Rb to Sn.

Results and discussion.— The resulting half-life measurements are illustrated in Fig. 2, compared with previous measurements and with the predictions of several theoretical models. The experimental half-lives follow very regular trends, as expected phenomenologically in nuclei with large Q values [33], but with the noticeable feature that the odd-even staggering of half-lives is significantly weakened crossing the $N = 82$ shell gap. This is a signature of the shell-structure of atomic nuclei and of the neutron-neutron pairing interaction, which is stronger in $N \leq 82$ nuclei (valence neutrons in the $h_{11/2}$ orbit) than in $N > 82$ nuclei (valence neutrons in the $f_{7/2}$ orbit).

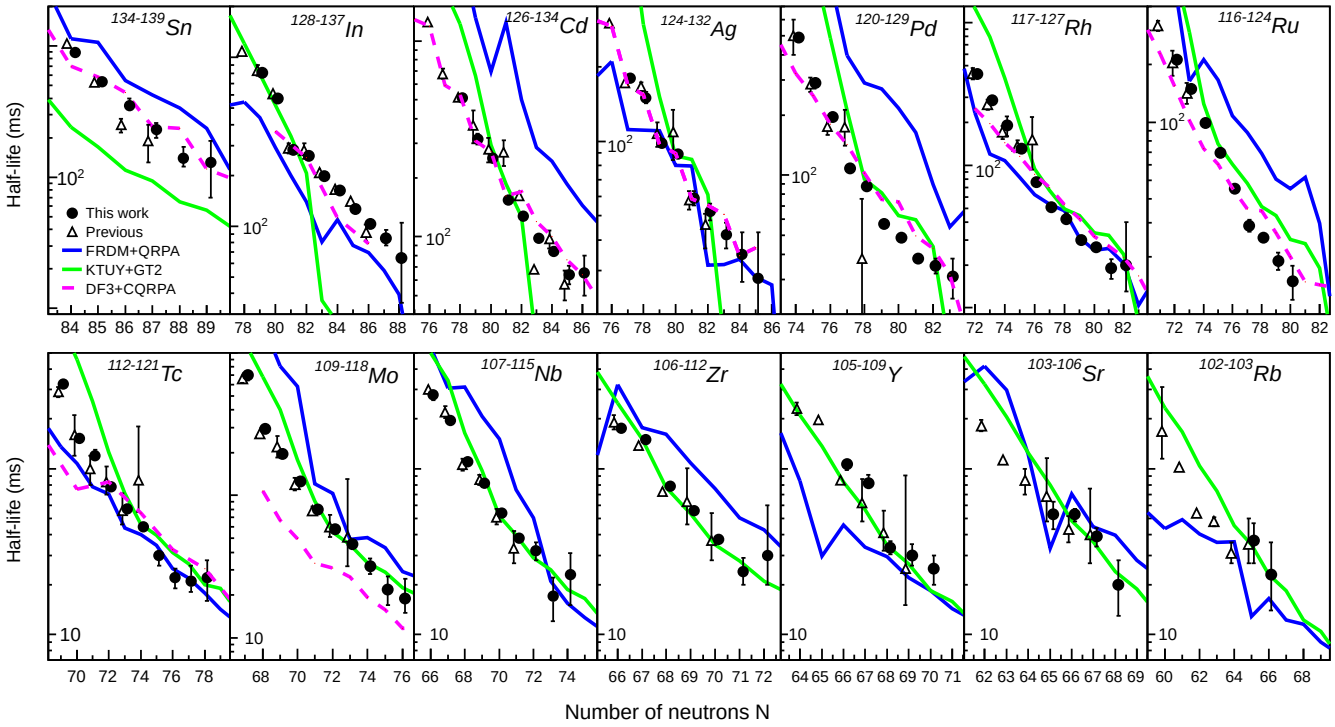

FIG. 2: (color online) β-decay half-lives determined in this work (solid circles) for a number of isotopic chains as a function of neutron number, compared with previous results [34] (open triangles) and the predictions of the models FRDM+QRPA (blue), KTUY + GT2 (green), and DF3+CQRPA (magenta) when available.

It is also clear that crossing the large $N = 82$ shell gap does not produce discontinuities in the half-life trends. These systematics, partially obscured in previous literature data probably by systematic errors, are now firmly established for In, Cd, Ag, and Pd isotopes, and can be interpreted by QRPA calculation as in Refs. [35–37]. In $N > 82$ nuclei, the g.s. to g.s. transition $\nu f_{7/2} \rightarrow \pi g_{9/2}$ is a first forbidden (ff) decay, and the GT transition $\nu f_{7/2} \rightarrow \pi f_{5/2}$ is largely blocked by the almost complete occupancy of the $\pi f_{5/2}$ orbital. The main GT-decay branch is $\nu g_{7/2} \rightarrow \pi g_{9/2}$, which populates excited states of daughter nuclei. Thus, the isobaric mass difference is not directly reflected in the Q value available for β decay. The half-life trends of In, Cd, and Ag isotopes agree very well with the DF3+CQRPA model predictions [37], which are applicable for nearly-spherical nuclei – In, Cd, and Ag isotopes are indeed expected to be spherical, based on several mass models. The agreement worsens for non closed-shell isotopes of lighter elements, suggesting that deformation in these isotopic chains is not negligible. The data presented here is important for the future development of the DF3+CQRPA model and its extention to non-spherical nuclei. Discrepancies by factor 3–4 between experimental half-lives and predictions of global models such as FRDM+QRPA [38] already observed for the more stable isotopes, persist further from stability. However, the general trend of FRDM+QRPA and experimental values is very similar, despite a systematic overestimation. This suggests a continuity of mass and decay properties between the studied nuclei and the previously known less exotic ones. Based on this comparison to theoretical models, we conclude that the data presented here show no evidence of nuclear structure changes capable to modify the gross properties of the nuclei we have studied. The sudden drop of half-lives observed of the KTUY+GT2 calculations [39, 40] when crossing of the $N = 82$ shell is not observed in the data. Since the Q_β values predicted by the KTUY and DF3 mass models are very similar, our data indicate a failure of the second generation of gross theory (GT2) employed to calculate half-lives rather than to the KTUY mass model.

The half-lives of the $N = 82$ nuclei are of particular interest to probe shell model calculations. The tendency to overestimate the half-life of ^{129}Ag reported in Refs. [41, 42], persists in the more exotic nuclei ^{128}Pd and ^{127}Rh (see Tab. I). However, in these calculations, the quenching factor of the GT operator ($q = 0.66$) was chosen to reproduce the half-life of ^{130}Cd (162±7 ms) reported in Ref. [43], which is longer than the one reported here (127±2 ms). The new $N = 82$ half-lives reveal that the calculated values are systematically longer by a nearly constant factor, with the only exception of

^{131}In. Assuming that the decay of $N = 82$ nuclei was dominated by GT transitions [42], such a constant factor could be approximately accounted by a different choice of the GT quenching factor. The value $q = 0.75$ extracted in this way agrees with the systematics of pf-shell nuclei [44] and neutron-deficient nuclei [45]. However, the new half-lives clearly indicate that the proton-hole nucleus ^{131}In is not following the trend expected from the shell-model calculations, an observation that calls for further investigation.

TABLE I: Comparison of the present $N = 82$ half-lives with previous measurements and the shell model calculations in Ref. [42].

Nucleus	Half-Life (ms)		
	This work	Previous	Shell Model
^{131}In	261(3)*	280(30) [46]	247.53
^{130}Cd	127(2)**	162(7) [43]	164.29
^{129}Ag	52(4)	46^{+5}_{-9} [47]	69.81
^{128}Pd	35(3)		47.25
^{127}Rh	20^{+20}_{-7}		27.98

*$T_{1/2}$ gated on γ-ray energy 2434 keV, **$T_{1/2}$ gated on γ-ray energies 451, 1669, and 1171 keV

Nucleosynthesis calculations.—The implications of the new half-lives for the r-process were investigated by conducting a fully dynamic reaction-network calculation [48] study that simulated a spherically-symmetric outflow from a neutron-rich stellar environment. The time evolution of matter density followed an early rapid exponential expansion with timescale τ and a later free expansion with a longer timescale approaching a constant velocity [49]. The initial proton-to-neutron ratio was set through the electron fraction Y_e, which, for matter consisting only of free neutrons n and protons p, is $Y_e = p/(n+p)$. In case of exploding stars, different mass zones (a star's layers of different density) have different initial entropy S, so that an explosion was simulated as a superposition of entropy components as in Refs. [50, 51]. Given the large uncertainties in current stellar hydrodynamical simulations, none of the above parameters was fixed to specific values. We choose instead to use a site-independent approach, where Y_e, τ, and S are free parameters determined by fitting the calculated abundance pattern to the observed solar one. This approach has proven to be valuable to study the underlying physics of the r-process and, avoiding assumptions on the astrophysics site, the extracted r-process path is defined from the new experimental nuclear physics data and the abundance observations. The parameter space extracted in this way for the KTUY mass model was Y_e=0.30(5), τ=80(20) ms, and S_{max} >400 (S in units of k_B baryon^{-1}). This space was strongly determined by the $A \approx 130$ peak, which is very sensitive to the r-process conditions. As an example, Fig. 3 shows the sensitivity of the r-process calculations to the parameter τ, for a fixed $Y_e = 0.3$. Given the parametrized astrophysical conditions, any confrontation between the resulting parameter space and the r-process site is clearly risky. However, since Y_e as low as $Y_e = 0.3$ have been recently realized in supernovae calculations [52], and since the limit $S_{max} \approx 100$ obtained in hydrodynamical simulations of supernova explosion is still uncertain, the parameter space extracted in this study is indeed compatible with high entropy ν-driven wind in core-collapse supernovae models. The features of the resulting r-process were very similar to the reported in Ref. [51], which is an in-depth study of the model. Calculations were also carried out in the parameter space resulting from the merging neutron stars calculation of Ref. [14]. In this case, the r-process is a superposition of Y_e components in the range $Y_e = 0.1 - 0.4$ and of entropy $S \sim 20$.

Implications for the r-process.—The impact of the new measurements on the calculated solar-abundance pattern is illustrated in Fig. 4, where two calculations are compared that differ only by the half-lives measured in this work. All the other nuclear structure data, as well as the astrophysics conditions, were the same. The new half-lives have a global impact on the calculated r-process abundances, and alleviate the underproduction of isotopes just below and above the $A \approx 130$ peak, which in the past required the introduction of shell-structure modifications [54–56]. A particularly beneficial effect of the new half-lives of the most neutron-rich isotopes of Ag, Cd, In, and Sn ($N > 82$), is to greatly improve the description of the abundance of rare earth elements, which is a prerequisite to study the universality of the r-process. The abundances of these elements are in fact coherently matching solar system and metal-poor stars.

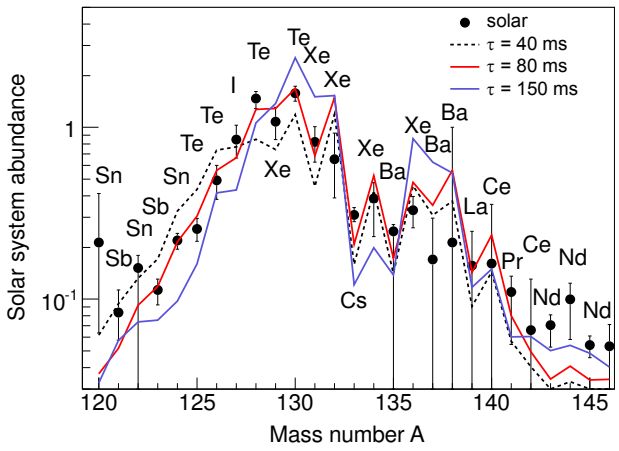

FIG. 3: (color online) Comparison between the solar r-process abundance distribution and reaction-network abundance calculations for different values of the expansion time τ.

The reduced nuclear physics uncertainty provides a new level of reliability for r-process calculations and their parametrized astrophysical conditions. In our calcula-

tions, the $A \approx 130$ and the rare earth elements peaks are produced mostly in $(n,\gamma) \rightleftarrows (\gamma,n)$ equilibrium, in agreement with Ref. [51]. Thus, the large beneficial impact of the experimental half-lives on r-process calculations supports the notion that the observed r-process abundance pattern may indeed result from the freezout of an $(n,\gamma) \rightleftarrows (\gamma,n)$ equilibrium. When using the FRDM mass model in the same astrophysical conditions, the r-process path moves to slightly more neutron-rich nuclei, but when calculations are fit to the solar abundance, they result in slightly different astrophysical conditions, which partially compensate the r-process path differences due to the different mass models. The effects of the new half-lives in the r-process calculations using KTUY, FRDM, and the HFB-14 mass models are very similar.

The solar system abundance pattern shown in Fig. 4 comprises contributions from many r-process events accumulated over time and consequently certain features may be averaged out. In contrast the photospheres of metal poor stars display the output of individual or very few r-process events since they belong to the earlier generation of stars. As mentioned in the introduction, recent observations for a number of metal poor stars demonstrated a robust production of Te [20, 21]. To study whether this finding implies the robustness of physical conditions in the r-process site we calculated elemental abundances for a range of parameters $\tau = 10 - 300$ ms, corresponding to different r-process conditions (different stars). As shown in Fig. 5, in all cases Te is indeed robustly produced in agreement with observation. Note, however, in the case of Te several stable isotopes are produced by the r-process. Although different r-process conditions shift the A 130 peak of the isotopic abundance distribution (compare Fig. 3) causing variations in the abundances of the different isotopes, these effects cancel each other leading to a robust elemental abundance of Te. However, the situation is different for the odd-Z elements I and Cs that only have one stable isotope (^{127}I and ^{133}Cs) and for Sn that lies on the tail of the peak. In these cases the elemental abundances retain their sensitivity to the r-process conditions. We conclude that (i) the robustness of Te is hardly connected to the robustness of the r-process conditions and (ii) the robustness of Te has a different nature than the one of rare earth elements, whose robustness was found also at the level of isotopic abundance distributions. Furthermore (iii) the elements Sn, Sb, I, Cs in metal-poor stars are indeed sensitive to the r-process conditions, and consequently the detection of these elements could provide new stringent constraints on individual r-process events.

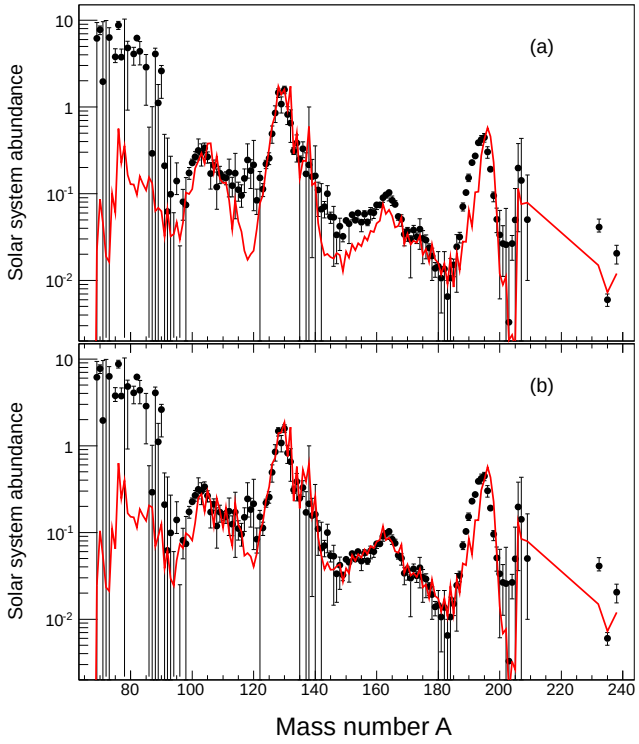

FIG. 4: (color online) Comparison between the r-process solar-system abundance pattern [17] and the abundances calculated (a) without and (b) with our new half-lives. In both calculations we input masses from the KTUY mass model [39] and reaction rates from the ReaclibV1 library [53]. The half-lives other than the ones we measured are from the FRDM+QRPA model [38].

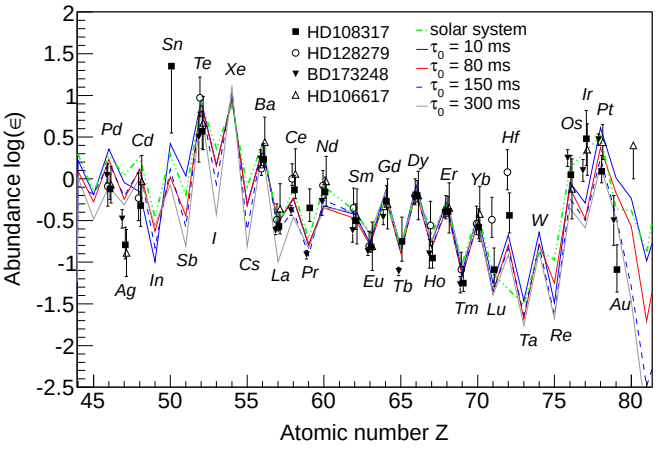

FIG. 5: (color online) Comparison between the elemental r-process abundance distributions in four metal-poor stars [20, 21], in the solar system, and calculated for a range of r-process conditions. All abundance distributions are normalized to the element Eu.

In the case of calculations for merging neutron stars, the impact of the new half-lives was found to be very small because the very short expected expansion time ($\tau \sim 10$ ms) drove the r-process path into very exotic regions. A larger, but nevertheless modest impact was found in case of larger expansion times ($\tau > 100$ ms), which is relevant for the r-process in the accretion disk around the black-hole remnant of binary neutron stars or

neutron star–black hole merger [57].

Conclusions.—The present study extends the limits of known β-decay half-lives to nuclei deep into the r-process path predicted for some of the most promising r-process sites such as ν-driven wind in core-collapse supernovae. The study demonstrates the persistence of shell effects and a robust half-lives systematics. The comparison to predictions of theoretical models shows no evidence of structural changes capable of modifying substantially the gross properties of the nuclei studied. Reaction-network calculations based on the new data reinforce the notion that the r-process abundance pattern could result from the freezout of an $(n,\gamma) \rightleftarrows (\gamma,n)$ equilibrium, and highlight the remarkable value of abundance observations in metal-poor stars and in particular of Te and the other elements contributing to the $A \approx 130$ r-process peak. The sensitivity of these elements to the r-process conditions may enable metal-poor stars observations to identify the exact conditions that triggered an individual r-process event.

Acknowledgment.—This work was carried out at the RIBF operated by RIKEN Nishina Center, RIKEN and CNS, University of Tokyo. The authors acknowledge discussion with Drs. Alfredo Estradé Vaz, and Volker Werner. We also acknowledge the EUROBALL Owners Committee for the loan of germanium detectors and the PreSpec Collaboration for the readout electronics of the cluster detectors. Part of the WAS3ABi was supported by the Rare Isotope Science Project which is funded by the Ministry of Education, Science and Technology (MEST) and National Research Foundation (NRF) of Korea. This work was partially supported by KAKENHI (Grant No. 25247045, No. 2301752, and No. 25800130), the RIKEN Foreign Research Program, the Spanish Ministerio de Ciencia e Innovación (Contracts No. FPA2009-13377-C02 and No. FPA2011-29854-C04), and the Hungarian Scientific Research Fund OTKA Contract No. K100835.

[1] F. Käppeler, H. Beer, and K. Wisshak, Rep. Progr. Phys. **52**, 945 (1989).
[2] F. Käppeler, R. Gallino, S. Bisterzo, and W. Aoki, Rev. Mod. Phys. **83**, 157 (2011).
[3] F. Hoyle, W. A. Fowler, G. R. Burbidge, and E. M. Burbidge, Science **124**, 611 (1956).
[4] J. J. Cowan, F.-K. Thielemann, and J. W. Truran, Phy. Rep. **208**, 267 (1991).
[5] M. Arnould, S. Goriely, and K. Takahashi, Phys. Rep. **450**, 97 (2007).
[6] S. E. Woosley and R. D. Hoffman, Astrophys. J. **395**, 202 (1992).
[7] K. Takahashi, J. Witti, and H.-T. Janka, Astron. Astrophys. **286**, 857 (1994).
[8] C. L. Fryer, F. Herwig, A. Hungerford, and F. X. Timmes, Astrophys. J. **646**, L131 (2006).
[9] S. Wanajo, M. Tamamura, N. Itoh, K. Nomoto, Y. Ishimaru, T. C. Beers, and S. Nozawa, Astrophys. J. **593**, 968 (2003).
[10] A. G. W. Cameron, Astrophys. J. **562**, 456 (2001).
[11] C. Winteler et al., Astrophys. J Lett. **750**, L22 (2012).
[12] J. A. Faber and F. A. Rasio, Living Rev. Relativ. **15**, 8 (2012).
[13] O. Korobkin, S. Rosswog, A. Arcones, and C. Winteler, Mon. Not. R. Astron. Soc. **426**, 1940 (2012).
[14] S. Wanajo et al., Astrophys. J Lett. **789**, L39 (2014), 1402.7317.
[15] C. Freiburghaus, S. Rosswog, and F.-K. Thielemann, Astrophys. J. **525**, L121 (1999).
[16] S. Wanajo, Astrophys. J. **666**, L77 (2007).
[17] S. Goriely, Astron. Astrophys. **342**, 881 (1999).
[18] H. R. Jacobson and A. Frebel, J Phys. G Nucl. Partic. **41**, 044001 (2014).
[19] C. Sneden, J. J. Cowan, and R. Gallino, Annu. Rev. Astron. Astr. **46**, 241 (2008).
[20] I. U. Roederer et al., Astrophys. J. **747**, L8 (2012).
[21] I. U. Roederer et al., Astrophys. J Suppl. S **203**, 27 (2012).
[22] A. Arcones and G. Martínez-Pinedo, Phys. Rev. C **83**, 045809 (2011), 1008.3890.
[23] H. Watanabe et al., Phys. Rev. Lett. **111**, 152501 (2013).
[24] H. Wang et al., Phys. Rev. C **88**, 054318 (2013).
[25] H. Watanabe et al., Phys. Rev. Lett. **113**, 042502 (2014).
[26] J. Taprogge et al., Phys. Rev. Lett. **112**, 132501 (2014).
[27] A. Jungclaus et al., Phys. Rev. Lett. **99**, 132501 (2007).
[28] I. Dillmann et al., Phys. Rev. Lett. **91**, 162503 (2003).
[29] S. Nishimura, Progr. Theor. Exp. Phys. **2012**, 03C006 (2012).
[30] P.-A. Söderström et al., Nucl. Instrum. Meth. B **317**, 649 (2013).
[31] Z. Y. Xu et al., Phys. Rev. Lett. **113**, 032505 (2014).
[32] Y. Shimizu et al. (2014), In manuscript.
[33] X. Zhang, Z. Ren, Q. Zhi, and Q. Zheng, J Phys. G Nucl. Phys. **34**, 2611 (2007).
[34] G. Audi et al., Chinese Phys. C **36**, 1157 (2012).
[35] T. Björnstad et al., Nucl. Phys. A **453**, 463 (1986).
[36] M. Hannawald et al., Phys. Rev. C **62**, 054301 (2000).
[37] I. N. Borzov et al., Nucl. Phys. A **814**, 159 (2008).
[38] P. Möller, B. Pfeiffer, and K.-L. Kratz, Phys. Rev. C **67**, 055802 (2003).
[39] H. Koura, T. Tachibana, M. Uno, and M. Yamada, Progr. Theor. Phys. **113**, 305 (2005).
[40] T. Tachibana, M. Yamada, and Y. Yoshida, Progr. Theor. Phys. **84**, 641 (1990).
[41] J. J. Cuenca-Garcıa et al., Eur. Phys. J A **34**, 99 (2007).
[42] Q. Zhi et al., Phys. Rev. C **87**, 025803 (2013).
[43] M. Hannawald et al., Nucl. Phys. A **688**, 578 (2001).
[44] G. Martínez-Pinedo, A. Poves, E. Caurier, and A. P. Zuker, Phys. Rev. C **53**, 2602 (1996).
[45] C. B. Hinke et al., Nature (London) **486**, 341 (2012).
[46] B. Fogelberg et al., Phys. Rev. C **70**, 034312 (2004).
[47] K.-L. Kratz et al., Hyperfine Interact. **129**, 185 (2000).
[48] M. J. Bojazi and B. S. Meyer, Phys. Rev. C **89**, 025807 (2014).
[49] I. V. Panov and H.-T. Janka, Astron. Astrophys. **494**, 829 (2009).
[50] C. Freiburghaus et al., Astrophys. J. **516**, 381 (1999).
[51] K. Farouqi et al., Astrophys. J. **712**, 1359 (2010).

TABLE II: Half-lives measured in the present work.

Nucleus	Half-Life (ms)	Nucleus	Half-Life (ms)	Nucleus	Half-Life (ms)	Nucleus	Half-Life (ms)	Nucleus	Half-Life (ms)
^{134}Sn	890(20)	^{132}Cd	82(4)	^{119}Rh	190(6)	^{118}Tc	30(4)	^{115}Nb	23(8)
^{135}Sn	515(5)	^{133}Cd	64(8)	^{120}Rh	131(5)	^{119}Tc	22(3)	^{106}Zr	175(7)
^{136}Sn	350(5)	^{134}Cd	65(15)	^{121}Rh	76(5)	^{120}Tc	21(5)	^{107}Zr	150(3)
^{137}Sn	230(30)	^{124}Ag	180(3)	^{122}Rh	51(6)	^{121}Tc	22(6)	^{108}Zr	785(2)
^{138}Sn	140^{+30}_{-20}	^{125}Ag	150(8)	^{123}Rh	42(4)	^{109}Mo	700^{+40}_{-60}	^{109}Zr	56(3)
^{139}Sn	130(60)	^{126}Ag	98(5)	^{124}Rh	30(2)	^{110}Mo	292(7)	^{110}Zr	37.5(20)
^{128}In	810(30)	^{127}Ag	89(2)	^{125}Rh	26.5(20)	^{111}Mo	196(5)	^{111}Zr	24.0(5)
^{129}In	570(10)	^{128}Ag	59(5)	^{126}Rh	19(3)	^{112}Mo	125(5)	^{112}Zr	30^{+30}_{-10}
^{130}In	284(10)	^{129}Ag	52(4)	^{127}Rh	20^{+20}_{-7}	^{113}Mo	80(2)	^{104}Y	198(20)
^{131}In	261(3)	^{130}Ag	42(5)	^{118}Ru	99(3)	^{114}Mo	58(2)	^{105}Y	107^{+6}_{-9}
^{132}In	198(2)	^{131}Ag	35(8)	^{119}Ru	69.5(20)	^{115}Mo	45.5(20)	^{106}Y	82^{+10}_{-5}
^{133}In	163(7)	^{132}Ag	28^{+15}_{-12}	^{120}Ru	45(2)	^{116}Mo	32(4)	^{107}Y	33.5(3)
^{134}In	126(7)	^{121}Pd	290(1)	^{121}Ru	29(2)	^{117}Mo	22(5)	^{108}Y	30(5)
^{135}In	103(5)	^{122}Pd	195(5)	^{122}Ru	25(1)	^{118}Mo	19^{+7}_{-4}	^{109}Y	25(5)
^{136}In	85^{+10}_{-8}	^{123}Pd	108(1)	^{123}Ru	19(2)	^{107}Nb	280(20)	^{103}Sr	53(10)
^{137}In	65^{+40}_{-30}	^{124}Pd	88(15)	^{124}Ru	15(3)	^{108}Nb	195(6)	^{104}Sr	53(5)
^{126}Cd	513(6)	^{125}Pd	57(10)	^{112}Tc	323(6)	^{109}Nb	110(6)	^{105}Sr	39(5)
^{127}Cd	330(20)	^{126}Pd	48.6(8)	^{113}Tc	152(8)	^{110}Nb	82(2)	^{106}Sr	20^{+8}_{-7}
^{128}Cd	245(5)	^{127}Pd	38(2)	^{114}Tc	120(10)	^{111}Nb	54(2)	^{102}Rb	37(10)
^{129}Cd	154.5(20)	^{128}Pd	35(3)	^{115}Tc	78(2)	^{112}Nb	38(2)	^{103}Rb	23^{+13}_{-9}
^{130}Cd	127(2)	^{129}Pd	31(7)	^{116}Tc	57(3)	^{113}Nb	32(4)		
^{131}Cd	98.0(2)	^{118}Rh	285(10)	^{117}Tc	44.5(30)	^{114}Nb	17(5)		

[52] M.-R. Wu, T. Fischer, L. Huther, G. Martínez-Pinedo, and Y.-Z. Qian, Phys. Rev. D **89**, 061303 (2014), 1305.2382.
[53] R. H. Cyburt et al., Astrophys. J. Suppl. **189**, 240 (2010).
[54] K.-L. Kratz et al., Astrophys. J. **403**, 216 (1993).
[55] B. Chen et al., Physics Letters B **355**, 37 (1995).
[56] M. Bender et al., Phys. Rev. C **80**, 064302 (2009).
[57] S. Wanajo, H.-T. Janka, and B. Müller, Astrophys. J Lett. **726** (2011).